Article

J. Biol. Regul. Homeost. Agents. 2024; 38(6): 4757–4770
https://doi.org/10.23812/j.biol.regul.homeost.agents.20243806.380

Short-chain Fatty Acids Inhibit NLRP3 Inflammasome to Alleviate Inflammation and Epithelial-mesenchymal Transition in Diabetic Nephropathy Rats via *GPR41/43*

Ningjun Shao[1], Kedan Cai[1], Yue Hong[1], Kaiyue Wang[1], Qun Luo[1,*], Lingping Wu[1,*]

[1]Department of Nephrology, Ningbo No.2 Hospital, 315010 Ningbo, Zhejiang, China
*Correspondence: nbluoqun@163.com (Qun Luo); wulingping1306@163.com (Lingping Wu)
Submitted: 15 January 2024 Revised: 28 February 2024 Accepted: 5 March 2024 Published: 1 June 2024

Background: The role of Short-chain fatty acids (SCFAs) and their G-protein-coupled receptors (GPRs) in mitigating diabetic nephropathy (DN) has been recognized. This study aimed to investigate the impact of SCFAs on inflammation in DN via G-protein-coupled receptors 41 and 43 (*GPR41/43*).

Methods: Human kidney tubular HK-2 cells were transfected to silence *GPR41/43* and treated with sodium acetate (Ac, 48 mmol/L)/sodium propionate (Pr, 24 mmol/L)/sodium butyrate (But, 8 mmol/L) under high glucose (HG, 30 mM) or normal glucose conditions. Rats were administered lentivirus solution to silence *GPR41/43* and streptozotocin (STZ, 60 mg/kg) to induce DN, followed by treatment with But (100 mmol/L). Diabetic symptoms and renal function were evaluated, kidney weight/body weight (KW/BW) was calculated, and renal histopathology was examined using hematoxylin-eosin, periodic acid-Schiff, and Masson staining. Quantitative real-time polymerase chain reaction, Western blot, enzyme-linked immunosorbent assay, and immunohistochemistry were employed to assess epithelial-mesenchymal transition (EMT)-related proteins, *GPR41*, *GPR43*, NLR family pyrin domain containing 3 (NLRP3), and inflammatory factor levels in HK-2 cells and kidney tissues.

Results: Ac/Pr/But reversed HG-induced downregulation in *GPR41*/*GPR43* and upregulation of *NLRP3*/tumor necrosis factor-α (*TNF-α*)/interleukin-18 (*IL-18*)/*IL-6*/*IL-1β* in HK-2 cells ($p < 0.001$). But attenuated HG-induced decrease in epithelial cadherin (E-cadherin) ($p < 0.001$) and increase in alpha-smooth muscle actin (α-SMA) ($p < 0.05$) in HK-2 cells. Silencing *GPR41/43* reversed the effects of But ($p < 0.05$). STZ induced diabetic symptoms, increased urine albumin level, serum creatinine/ blood urea nitrogen (BUN) level, KW/BW, α-SMA, NLRP3, and inflammatory factor levels in kidney tissues, exacerbated kidney morphology, and downregulated E-cadherin and *GPR41*/*GPR43* in kidney tissues in rats ($p < 0.001$). But attenuated these effects of STZ, which were reversed by silencing *GPR41/43* ($p < 0.05$).

Conclusions: SCFAs inhibit NLRP3 inflammasome activation, thus alleviating inflammation and EMT in DN by upregulating *GPR41/43*.

Keywords: short chain fatty acids; NLRP3; epithelial-mesenchymal transition; diabetic nephropathy; *GPR41/43*

Introduction

Diabetic nephropathy (DN) is a severe chronic microvascular complication of diabetes characterized by various pathological abnormalities, including increased inflammation, accumulation of reactive oxygen species (ROS), proteinuria, and gradual decline in renal function [1,2]. Given its high incidence among end-stage renal disease (ESRD) cases and its primary role as an inducer of ESRD, DN represents a significant public health challenge worldwide [2]. Despite advancements in therapeutic methods that alleviate DN symptoms and slow its progression to ESRD, the cure rate of patients remains unsatisfactory [3].

Chronic inflammation plays a vital role in the onset and progression of DN in extensive experimental and theoretical studies [4]. In addition to its direct effects, inflammation has been implicated in facilitating other pathological processes in DN, such as renal fibrosis, which can be driven by the epithelial-mesenchymal transition (EMT) of tubular epithelial cells [5]. The concurrence of inflammation and fibrosis in DN often leads to the development of chronic kidney disease (CKD), which may ultimately progress to ESRD [5]. Therefore, investigating the mechanisms underlying renal inflammation and EMT in DN holds promise for shedding light on its pathogenesis and developing novel treatment strategies.

The induction and perpetuation of chronic inflammation in DN are closely associated with the activation of NOD-like receptors (NLRs) and intracellular pattern recognition receptors (PRRs) by intracellular and extracellular danger-associated molecular patterns and pathogen-associated molecular patterns [6]. NLR family pyrin domain containing 3 (NLRP3) is activated in the form of the NLRP3 inflammasome, driving the progression of DN, and

Journal of
BIOLOGICAL REGULATORS
and Homeostatic Agents

targeting it is considered a potential therapeutic option for DN [7]. The NLRP3 inflammasome consists of NLRP3, pro-Caspase-1, and apoptosis-associated speck-like protein containing a CARD (ASC) [8]. Its activation leads to the cleavage of caspase-1, resulting in the activation of inflammatory effectors interleukin-1β (IL-1β) and IL-18, thereby influencing the microinflammatory state of DN at multiple levels [9,10].

Long-term dysbiosis triggers a persistent systemic inflammatory state and contributes to the development of DN [11] through the interplay between the kidney and intestine, a phenomenon termed the "gut-kidney axis" [12]. Mechanistically, dysbiosis-induced enhanced permeability of the intestinal wall permits the translocation of significant quantities of bacteria and toxins into the bloodstream, thereby activating the monocyte-macrophage system and promoting the release of numerous cytotoxic substances, which exacerbate inflammatory organ damage, including in the kidney [13]. The primary mediators implicated in the "gut-kidney axis" are metabolites of intestinal flora [14]. Short-chain fatty acids (SCFAs), predominantly butyrate, propionate, and acetate, are essential metabolites formed by intestinal flora through the fermentation of undigested carbohydrates and dietary fiber [15,16]. SCFAs reduce renal fibrosis in CKD by inhibiting the NLRP3 inflammasome activation [17]. Moreover, the protective role of SCFAs in DN against renal inflammation and fibrosis has been demonstrated in several studies [18,19]. SCFAs also ameliorate inflammatory or fibrotic responses induced by high glucose (HG) in renal tubular epithelial cells [20]. However, whether SCFAs alleviate DN *in vivo* by suppressing tubular epithelial cell inflammation and EMT requires further validation.

G-protein-coupled receptors 41 and 43 (*GPR41* and *GPR43*) are a pair of cell surface G-protein-coupled receptors (GPRs) involved in the regulation of inflammation [21]. SCFAs upregulate *GPR43* to ameliorate DN and associated inflammation and fibrosis [18]. Additionally, SCFAs can inhibit tumor necrosis factor-α (*TNF*-α)-induced inflammation in renal cortical epithelial cells by activating *GPR41* and *GPR43* [22]. However, whether SCFAs regulate NLRP3 in renal tubular epithelial cells via *GPR41/43* to alleviate DN remains to be elucidated.

This study aimed to elucidate the effect and mechanisms of SCFAs in the onset and progression of DN, explore new therapeutic avenues for DN, and establish a novel theoretical framework for delaying renal damage and improving patient prognosis.

Materials and Methods

Cell Culture

The human kidney tubular cell line HK-2 (CRL-2190) from the American Type Culture Collection (ATCC, Manassas, VA, USA) was cultured in Dulbecco's Modified Eagle's Medium (DMEM, 11966025, Thermo Fisher, Waltham, MA, USA) supplemented with 10% fetal bovine serum (FBS, 30-2020, ATCC, Manassas, VA, USA) in a humidified atmosphere with 5% CO_2 at 37 °C. The HK-2 cells were sub-cultured every four days, with the medium changed every 2 days, and transferred to an FBS-deprived medium for 24 hours before experiments. Authentication of HK-2 cells was performed using short tandem repeat (STR) analysis, and they were confirmed free of mycoplasma contamination.

Cell Transfection and Treatment

Small interfering RNA against *GPR41* (siGPR41, A01010) and *GPR43* (siGPR43, A01010) were obtained from Genepharma (Shanghai, China). Three different siRNA were used for each target gene: siGPR41#1: 5′-ATGGATTCTGCCCTTCATCTTCT-3′, siGPR41#2: 5′-CTGAATACTGGGGAAATGCAACC-3′, siGPR41#3: 5′-CCCTGTGTATTACCAGTTACTGC-3′; siGPR43#1: 5′-CGGCTTCTACAGCAGTATCTACT-3′, siGPR43#2: 5′-ACCAAATCACCTGCTATGAGAAC-3′, siGPR43#3: forward, 5′-CCAGCCTGGATCCATTATT-3′; reverse, 5′-AAUAAUGGAUCCAGGCUGG-3′. A small interfering RNA negative control (siNC, A01010) was also included.

The transfection of siGPR41, siGPR43, and siNC into HK-2 cells at approximately 80% confluence was performed using Lipofectamine™ 3000 Transfection Reagent (L3000015, Thermo Fisher, Waltham, MA, USA). Sodium acetate (Ac, CH_3COONa, $\geq$99%; S2889, Sigma-Aldrich, Saint Louis, MO, USA), sodium propionate (Pr, CH_3CH_2COONa, $\geq$99%; V900330, Sigma-Aldrich, Saint Louis, MO, USA), sodium butyrate (But, $CH_3CH_2CH_2COONa$, 99%; V900464, Sigma-Aldrich, Saint Louis, MO, USA), and glucose ($C_6H_{12}O_6$, $\geq$98%; HY-B0389, MedChemExpress, Monmouth Junction, NJ, USA) were dissolved in water separately. Untransfected HK-2 cells were treated with 48 mmol/L Ac, 24 mmol/L Pr, or 8 mmol/L But for 2 hours, while transfected cells were treated with 8 mmol/L But for 2 hours. Subsequently, all cells were stimulated with high glucose (HG, 30 mM) for 24 hours. Normal glucose (NG) at 5.6 mM was used as a control treatment for 24 hours of cell induction (**Supplementary Fig. 1**) [18].

Establishment of the Lentiviral Vector Carrying Short Hairpin RNA against GPR41/43 (shGPR41/43)

The lentiviral vector expressing rat sh*GPR41/43* and short hairpin RNA negative control (shNC) were obtained from Genepharma (Shanghai, China). The sequences for sh*GPR41* were as follows: forward- 5′-GTGGACTATCCTTGATGATAA-3′, reverse- 5′-TTATCATCAAGGATAGTCCAC-3′. The sequences for sh*GPR43* were: forward- 5′-GCCCTCTGGGCTTCCATAAAT-3′, reverse- 5′-

ATTTATGGAAGCCCAGAGGGC-3′. A total volume of 100 μL of lentivirus solution at a titer of 10^7 transfection units (TU)/mL was injected into the rat kidney once.

Animal Models and Administration Method

Male Sprague-Dawley (SD) rats (n = 60), aged 8–10 weeks and weighing 200–220 g, were obtained from Vital River (Beijing, China) and housed in an animal facility under controlled conditions: temperature of 23 ± 2 °C, humidity of 50%, and a 12-hour light/dark cycles, with *ad libitum* access to water and food. Ethical approval was obtained from the Ethics Committee of Zhejiang Baiyue Biotech Co., Ltd. for Experimental Animals Welfare (approval number: ZJBYLA-IACUC-20220601).

Streptozotocin (STZ, $C_8H_{15}N_3O_7$, ≥99%; HY-13753, MedChemExpress, Monmouth Junction, NJ, USA) was dissolved in water. One week after injection of the lentivirus solution, rats underwent a 12-hour fasting period and were intraperitoneally injected with STZ at a dose of 60 mg/kg to induce diabetes mellitus [23]. An equal volume of peanut oil was used as a control for STZ treatment in the control group. Blood samples were collected from the tail vein 72 hours after STZ injection and fasting blood glucose concentrations were measured using a blood glucose monitor (ACCU-CHEK Performa, Roche, Basel, Switzerland). Diabetes mellitus was diagnosed if the blood glucose level was ≥16.7 mmol/L [24]. 24-hour urine specimens were collected three weeks later, and urine albumin ≥30 mg/day confirmed the successful establishment of the DN model [23]. Following successful model establishment, rats were orally administered 100 mmol/L But daily for 12 weeks (**Supplementary Fig. 1**) [18].

Grouping

Rats (n = 60) were randomly assigned to groups using the random number table method (n = 10/group): the normal control (NC), DN, DN+But, DN+But+shNC, DN+But+shGPR41, and DN+But+shGPR43 groups. Rats in the NC group received peanut oil injection, while those in other groups were injected with STZ at 60 mg/kg. All groups except NC and DN groups were administered 100 mmol/L But. Rats in the DN+But+shNC, DN+But+shGPR41, and DN+But+shGPR43 groups were also injected with the corresponding lentivirus solution. Following But administration, rats were anesthetized with 1% Pelltobarbitalum Natricum (150 mg/kg) and euthanized by cervical dislocation.

Diabetic Symptoms

Blood glucose levels, 24-hour food and water intake, and 24-hour urine volume of the rats were monitored at 0, 3, 5, 7, 9, and 11 weeks after DN induction. Additionally, the body weight of the rats was measured weekly for 12 weeks following DN induction. Serum insulin levels were assessed 12 weeks post-DN induction using enzyme-linked immunosorbent assay (ELISA), as described in a subsequent section.

Renal Histopathology

Rats were euthanized immediately after 12 weeks of But administration (using the previously described method of euthanasia). Kidneys from the rats were fixed in 10% formalin (F301880, Aladdin, Shanghai, China) and decalcified using 5% nitric acid (438073, Sigma-Aldrich, Saint Louis, MO, USA). After dehydration in 50%–95% ethanol (E111991, Aladdin, Shanghai, China) and clarification with xylene (X112054, Aladdin, Shanghai, China), the kidneys were embedded in paraffin, and 4 μm-thick renal sections were prepared. Subsequently, the sections were deparaffinized and treated with ethanol.

Hematoxylin & Eosin (H&E) Staining

For H&E staining, sections were stained with hematoxylin (1 mL, H8070, Solarbio, Beijing, China) for 8 minutes. Subsequently, the sections were differentiated in a 5% acetic acid solution (A291611, Aladdin, Shanghai, China) and rinsed in running water. This was followed by treatment with 0.5% Ammonium Hydroxide (A299569, Aladdin, Shanghai, China) and an additional rinse. Finally, the sections were stained with 0.5% eosin (E292725, Aladdin, Shanghai, China) for 3 minutes.

Periodic Acid-Schiff (PAS) Staining

To assess glomerulosclerosis via PAS staining, corresponding kits (PAS, G1280, Solarbio, Beijing, China) were utilized. Briefly, sections were stained with PAS oxidizer for 10 minutes and then rinsed. Subsequently, Schiff staining solution was added for a 10-minute staining of the sections, followed by a 3-minute counterstaining with hematoxylin.

Masson Staining

Masson staining kits (G1340, Solarbio, Beijing, China) were utilized to detect collagen deposition and interstitial lesions. In brief, sections were stained with hematoxylin for 5 minutes, followed by differentiation and bluing induction. Subsequently, ponceau magenta was applied to stain the sections for 5 minutes. After a 1-minute wash with acetic acid solution and phosphomolybdic acid solution, respectively, the sections were dyed in aniline blue solution for 2 minutes.

Images of the stained sections were captured under a light microscope (WMS-1033, WUMO, Shanghai, China) at ×400 magnification. To quantify the PAS-positive area in glomeruli reflecting the mesangial index, 20 glomeruli were randomly selected from each group in PAS-stained sections and subjected to data analysis using ImageJ software (version 1.46, National Institutes of Health, Bethesda, MD, USA) [24].

Journal of
BIOLOGICAL REGULATORS
and Homeostatic Agents

Western Blot Analysis

Total protein extraction and quantification in HK-2 cells and renal tissues were performed using Radioimmunoprecipitation assay (RIPA) lysis buffer (P0013C, Beyotime, Shanghai, China) and a Bicinchoninic Acid (BCA) Protein Assay Kit (7780S, CST, Danvers, MA, USA), respectively. Following protein separation by sodium dodecyl sulphate polyacrylamide gel electrophoresis (SDS-PAGE, P0012A, Beyotime, Shanghai, China) and transfer onto polyvinylidene difluoride (PVDF) membranes (88518, Thermo Fisher, Waltham, MA, USA), the membranes were blocked with 5% skim milk for 2 hours at room temperature (RT), and incubated with primary antibodies (overnight at 4 °C) from Abcam (Cambridge, UK): epithelial cadherin (E-cadherin, ab231303, 97 kDa, 1:1000), alpha-smooth muscle actin (α-SMA, ab108424, 32 kDa, 1:1000), and glyceraldehyde-3-phosphate dehydrogenase (GAPDH, internal control, ab22555, 36 kDa, 1:1000).

Subsequently, membranes were washed with Tris-buffered saline with 0.1% Tween-20 (TBST, Solarbio, Beijing, China) before incubation with secondary antibodies (Goat Anti-Mouse IgG (AP124, 1:3000) or Goat Anti-Rabbit IgG (AP132, 1:3000) from Sigma-Aldrich (Saint Louis, MO, USA)) for 1 hour at room temperature. Protein bands were detected using Chemiluminescent Substrate (34577, Thermo Fisher, Waltham, MA, USA), and images were captured with the Odyssey® M Imaging System (LI-COR Biosciences, Lincoln, NE, USA). The results were analyzed using ImageJ software (version 1.46, National Institutes of Health, Bethesda, MD, USA).

Quantitative Real-time Polymerase Chain Reaction (qRT-PCR)

After total RNA extraction from HK-2 cells and kidney tissues using an RNA extraction kit (R1200, Solarbio, Beijing, China) and quantification with a UV spectrophotometer (DR6000, HACH, Shanghai, China), complementary DNA (cDNA) synthesis by reverse transcription was performed using the Primescript™ RT reagent Kit (RR037A, TaKaRa, Osaka, Japan). Subsequently, cDNA was amplified in a StepOne Plus real-time PCR system (4376600, Thermo Fisher, Waltham, MA, USA) using SYBR Premix Ex Taq II (RR820A, Takara, Osaka, Japan). Messenger RNA (mRNA) levels of *GPR41*, *GPR43*, *NLRP3*, *TNF-α*, *IL-18*, *IL-6*, and *IL-1β* were quantitated using the $2^{-\Delta\Delta Ct}$ method with *GAPDH* as an internal reference [23]. The primers used for HK-2 cells and renal tissues are listed in **Supplementary File 1**.

Enzyme-linked Immunosorbent Assay (ELISA)

24-hour urine samples from the rats were utilized to detect urine albumin levels at 24 hours, 3, 5, 7, 9, and 11 weeks following DN induction using a rat albumin ELISA kit (JL15579, Jianglaibio, Shanghai, China). Briefly, 50 µL standard/sample was added to appropriate wells, followed by a 1-hour incubation with 100 µL of horseradish peroxidase (HRP)-labelled antibody at 37 °C. Each well was washed with 350 µL of washing buffer, followed by 15-minute incubation with 50 µL of substrates A and B at 37 °C. After the addition of 50 µL Stop Solution, the optical density (OD) was measured using a microplate reader (1215D29, Thomas Scientific, Swedesboro, NJ, USA) at 450 nm.

Under anesthesia using 1% Pelltobarbitalum Natricum (45 mg/kg, P3761, Sigma-Aldrich, Saint Louis, MO, USA), blood samples were collected from rats via retroorbital puncture and centrifuged (10,000 ×g, 4 °C, 10 minutes) to obtain the supernatant. Serum insulin, creatinine, and blood urea nitrogen (BUN) levels were determined using ELISA kits (QY-R2097 and QY-R2120, QIYI, Shanghai, China; FT-PD6164S, FANTAI, Shanghai, China). Samples were added to wells, and each well was then incubated with 50 or 100 µL ELISA Reagent for 30 minutes or 1 hour at 37 °C, followed by washing. Subsequently, 50 µL of each Developer A and B was added to each well and incubated for 15 minutes in the dark at 37 °C. After adding 50 µL Stop Solution, absorbance was measured using a microplate reader at 450 nm.

Following cervical dislocation, the kidneys of the rats were immediately dissected, washed in ice-cold saline (IN9000, Solarbio, Beijing, China), and weighed. The kidney weight/body weight (KW/BW) was then calculated. Determination of TNF-α, IL-18, and IL-1β contents in kidney tissues was performed using ELISA kits (KRC3011, KRC2341, Thermo Fisher, Waltham, MA, USA; IQR-IL1b-1, RayBiotech, Atlanta, GA, USA). For TNF-α and IL-18 contents, 100 µL standards, controls, or samples were added to each well, followed by the addition of required buffer, and incubation for 2 hours at room temperature. After washing, each well was incubated with 100 µL Rt TNF-α/IL-18 Biotin Conjugate solution (1 hour), 100 µL 1X Streptavidin-HRP solution (30 minutes), and 100 µL Stabilized Chromogen (30 minutes) in the dark. The reaction was then stopped by adding 100 µL of Stop Solution, and the OD value was obtained using a microplate reader at 450 nm. For IL-1β content, 25 µL standards or samples were added to each well and incubated overnight at 4 °C. A 1-hour incubation with 25 µL Detection Antibody at room temperature, followed by the addition of 25 µL IQELISA Detection Reagent, was performed in each well. Subsequently, 15 µL Primer solution and 10 µL of PCR master mix were added, and real-time PCR was conducted. The PCR reaction conditions was set as follows: initial denaturation (95 °C, 2 minutes), followed by 35 cycles of denature (95 °C, 15 second) and annealing, extension, and fluorescence detection (60 °C, 25 second).

Immunohistochemistry

Immunohistochemistry staining was performed to quantify NLRP3 expression in kidney tissues. Samples

were deparaffinized and rehydrated, followed by treatment with 3% hydrogen peroxide (H_2O_2, H414630, Aladdin, Shanghai, China) for 30 minutes at 37 °C to block endogenous peroxidase activity. After rinsing in phosphate-buffered saline (PBS, C0221A, Beyotime, Shanghai, China), antigen retrieval was achieved by incubating the samples in sodium citrate buffer (pH = 6.0, J61815.AK, Thermo Fisher, Waltham, MA, USA) for 10 minutes. Subsequently, tissue sections were blocked with 5% bovine serum albumin (A116563, Aladdin, Shanghai, China) for 1 hour to minimize non-specific binding.

The primary antibody against NLRP3 (orb101128, 1:200, Biorbyt, Wuhan, China) was then applied and incubated overnight at 4 °C. Subsequently, the sections were incubated with HRP-conjugated secondary antibody (ab6721, 1:1000, Abcam, Cambridge, UK) for 30 minutes at room temperature. Immunoreactivity was visualized by treating the sections with diaminobenzidine (DAB) solution (D106469, Aladdin, Shanghai, China), followed by counterstaining with hematoxylin and dehydration. The stained sections were observed under a light microscope (WMS-1033, WUMO, Shanghai, China) at ×400 magnification.

Statistical Analysis

Data analysis was conducted using GraphPad Prism 8.0 (GraphPad Software, San Diego, CA, USA), and results are presented as mean ± standard deviations. Two-group and multi-group comparisons were conducted using the independent sample *t*-test and One-way analysis of variance, respectively, followed by a post hoc Tukey test for multiple comparisons. A p-value < 0.05 was considered statistically significant.

Results

SCFAs Reverses the Role of HG in Inhibiting GPR41/GPR43 and Inducing NLRP3 Inflammasome Activation in HK-2 Cells

To investigate the impact of SCFAs on *GPR41*/*GPR43* and NLRP3 inflammasome activation in HG-stimulated HK-2 cells *in vitro*, cells were pre-treated for 2 hours with 48 mmol/L acetate (Ac), 24 mmol/L propionate (Pr), or 8 mmol/L butyrate (But), followed by a 24-hour stimulation with 30 mM HG. The results of qRT-PCR revealed that *GPR41* and *GPR43* were down-regulated, while *NLRP3*, *TNF-α*, *IL-18*, *IL-6*, and *IL-1β* were upregulated in HK-2 cells after HG stimulation (Fig. 1A–G, $p < 0.001$). However, the effect of HG was counteracted by Ac, Pr, or But (Fig. 1A–G, $p < 0.001$). Thus, SCFAs activate *GPR41*/*GPR43*, inhibiting NLRP3 inflammasome activation in HG-stimulated HK-2 cells. Notably, the effect of 8 mmol/L But was the most pronounced and was selected for subsequent experiments.

Silencing of GPR41/GPR43 Reverses the Attenuating Effect of But in HG-induced EMT in HK-2 Cells

Transfection with si*GPR41* (#1, #2, #3) downregulated *GPR41* levels in HK-2 cells (Fig. 1H, $p < 0.001$). Similarly, *GPR43* expression in HK-2 cells was inhibited by si*GPR43* transfection (Fig. 1I, $p < 0.01$). si*GPR41*#3 and si*GPR43*#1 exhibited the best transfection efficiency and were selected for subsequent experiments.

Compared to the NG group, levels of E-cadherin decreased while α-SMA levels were elevated in the HG group (Fig. 1J,K, $p < 0.01$). Furthermore, But treatment reversed the effects of HG on E-cadherin and α-SMA expressions (Fig. 1J,K, $p < 0.05$). However, *GPR41*/*GPR43* knockdown attenuated the reversal role of But; E-cadherin expression was reduced, and α-SMA expression was increased in the HG+But+siGRP41 and HG+But+siGRP43 group compared to the HG+But+siNC group (Fig. 1J,K, $p < 0.05$). Consequently, *GPR41*/*GPR43* silencing reversed the attenuating effect of But on HG-induced EMT in HK-2 cells.

GPR41/GPR43 Silencing Reverses the Attenuating Effect of But on HG-induced GPR41/GPR43 Inhibition and NLRP3 Inflammasome Activation in HK-2 Cells

As shown in Fig. 2A–G, HG downregulated *GPR41* and *GPR43* while upregulating *NLRP3*, *TNF-α*, *IL-18*, *IL-6*, and *IL-1β* in HK-2 cells ($p < 0.001$), which was counteracted by But stimulation ($p < 0.001$). Knockdown of *GPR41*/*GPR43* mitigated the reversal effect of But ($p < 0.001$). Consequently, *GPR41*/*GPR43* silencing reversed the attenuating effect of But on HG-induced inflammation in HK-2 cells.

GPR41/GPR43 Silencing Reverses the Effect of But on Diabetic Symptoms and Renal Dysfunction in DN Rats

To investigate how *GPR41*/*GPR43* knockdown affects the role of But in DN rats, the rats received a single sterile intraperitoneal injection of 60 mg/kg STZ to induce DN rat models. One week prior to modeling, some rats were injected with a lentivirus solution silencing *GPR41*/*GPR43* directly into the kidney. Others were administered daily with 100 mmol/L But for 12 weeks following the modeling.

Compared to the NC group, the DN group exhibited higher blood glucose levels at 11 weeks (Fig. 3A, $p < 0.001$). However, But administration significantly reduced blood glucose levels in the DN group (Fig. 3A, $p < 0.001$). This hypoglycemic effect of But was diminished by *GPR41*/*GPR43* knockdown (Fig. 3A, $p < 0.001$). Additionally, the DN group showed increased urine volume, food intake, and water intake at 11 weeks and increased body weight at 12 weeks compared to the NC group (Fig. 3B–E, $p < 0.001$). However, these parameters

Journal of
BIOLOGICAL REGULATORS
and Homeostatic Agents

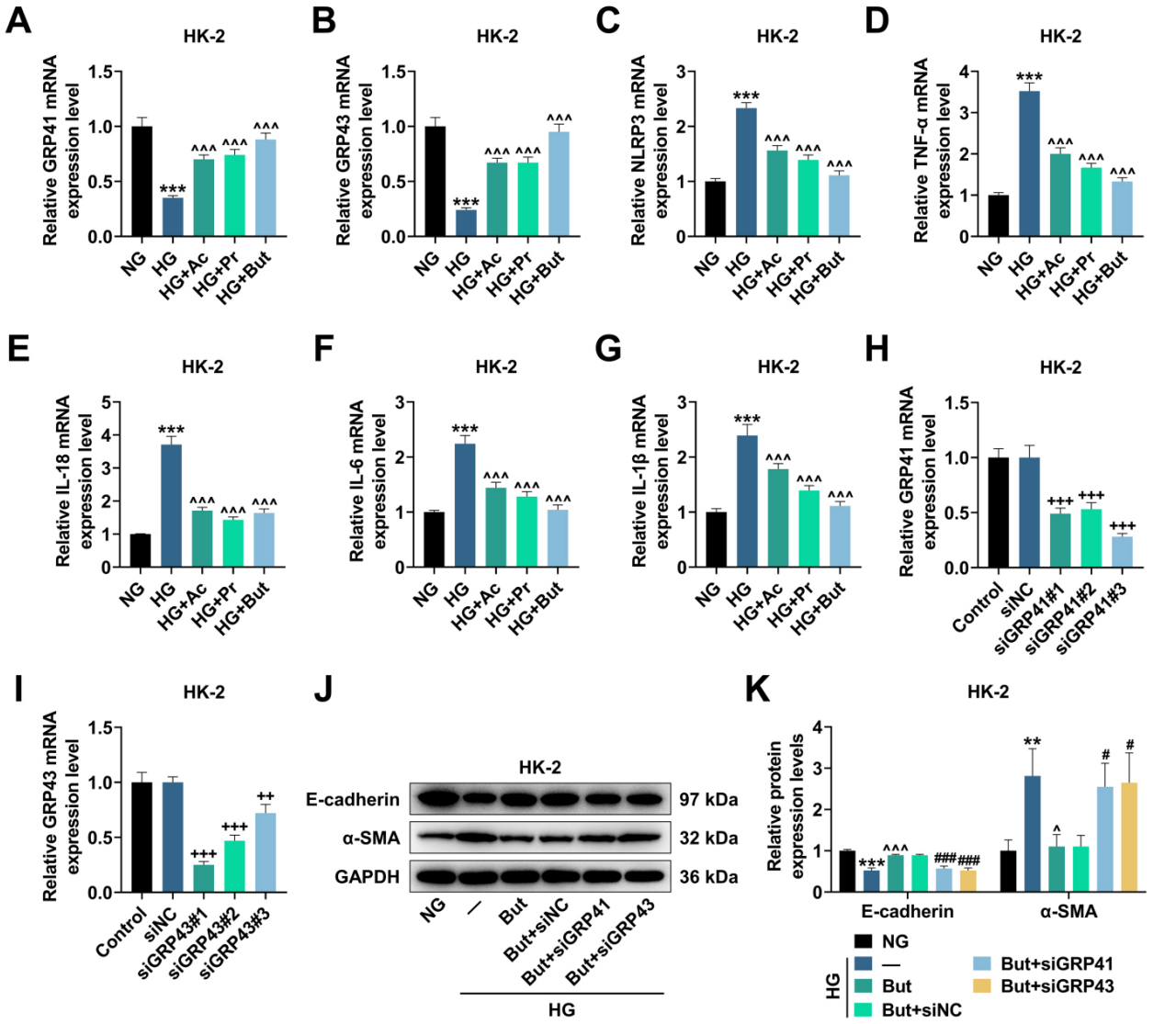

Fig. 1. SCFAs activate *GPR41*/*GPR43* and inhibit NLRP3 inflammasome activation, and *GPR41*/*GPR43* silencing reverses the attenuating effect of But in EMT in HG-induced HK-2 cells. (A–G) HK-2 cells were pretreated with Ac, Pr, or But for 2 hours and then stimulated with HG for 24 hours. The expression levels of *GPR41*, *GPR43*, *NLRP3*, TNF-α, *IL-18*, *IL-6*, and *IL-1*β in the HK-2 cells were determined using qRT-PCR, with *GAPDH as* a reference gene. (H,I) The transfection efficiency of HK-2 cells with si*GPR41* (si*GPR41*#1, si*GPR41*#2, and si*GPR41*#3) and si*GPR43* (si*GPR43*#1, si*GPR43*#2, and siGPR43#3) was assessed using qRT-PCR, with *GAPDH* as a loading control. (J,K) HK-2 cells were transfected with either siNC, si*GPR41*, or siGPR43 and then treated with But for 2 hours, followed by stimulation with HG for 24 hours. The expressions of EMT-related proteins, including E-cadherin and α-SMA, were analyzed using Western blot, with GAPDH as an internal standard. $^{**}p < 0.01$, $^{***}p < 0.001$ vs. NG; $^{\wedge}p < 0.05$, $^{\wedge\wedge\wedge}p < 0.001$ vs. HG; $^{++}p < 0.01$, $^{+++}p < 0.001$ vs. siNC; $^{\#}p < 0.05$, $^{\#\#\#}p < 0.001$ vs. HG+But+siNC. n = 3. But, 8 mmol/L sodium butyrate; EMT, epithelial-mesenchymal transition; HG, 30 mM high glucose; NG, 5.6 mM normal glucose; Ac, 48 mmol/L sodium acetate; Pr, 24 mmol/L sodium propionate; SCFA, Short-chain fatty acid; *GPR41/43*, G-protein-coupled receptor 41/43; NLRP3, NLR family pyrin domain containing 3; *TNF-*α, tumor necrosis factor-α; *IL-18/6/1*β, interleukin-18/6/1β; qRT-PCR, quantitative real-time polymerase chain reaction; GAPDH, glyceraldehyde-3-phosphate dehydrogenase; E-cadherin, epithelial cadherin; α-SMA, alpha-smooth muscle actin; siGPR41/43, small interfering RNA against *GPR41/43*; siNC, small interfering RNA negative control.

were reduced following But administration (Fig. 3B–E, $p < 0.05$). Nevertheless, the attenuating effect of But was weakened by *GPR41*/*GPR43* knockdown (Fig. 3B–E, $p < 0.001$). Conversely, serum insulin levels were lower in the DN group than in the NC group (Fig. 3F, $p < 0.001$). However, But administration restored the serum insulin levels in the DN group (Fig. 3F, $p < 0.001$), but this effect was offset by *GPR41*/*GPR43* knockdown (Fig. 3F, $p < 0.001$).

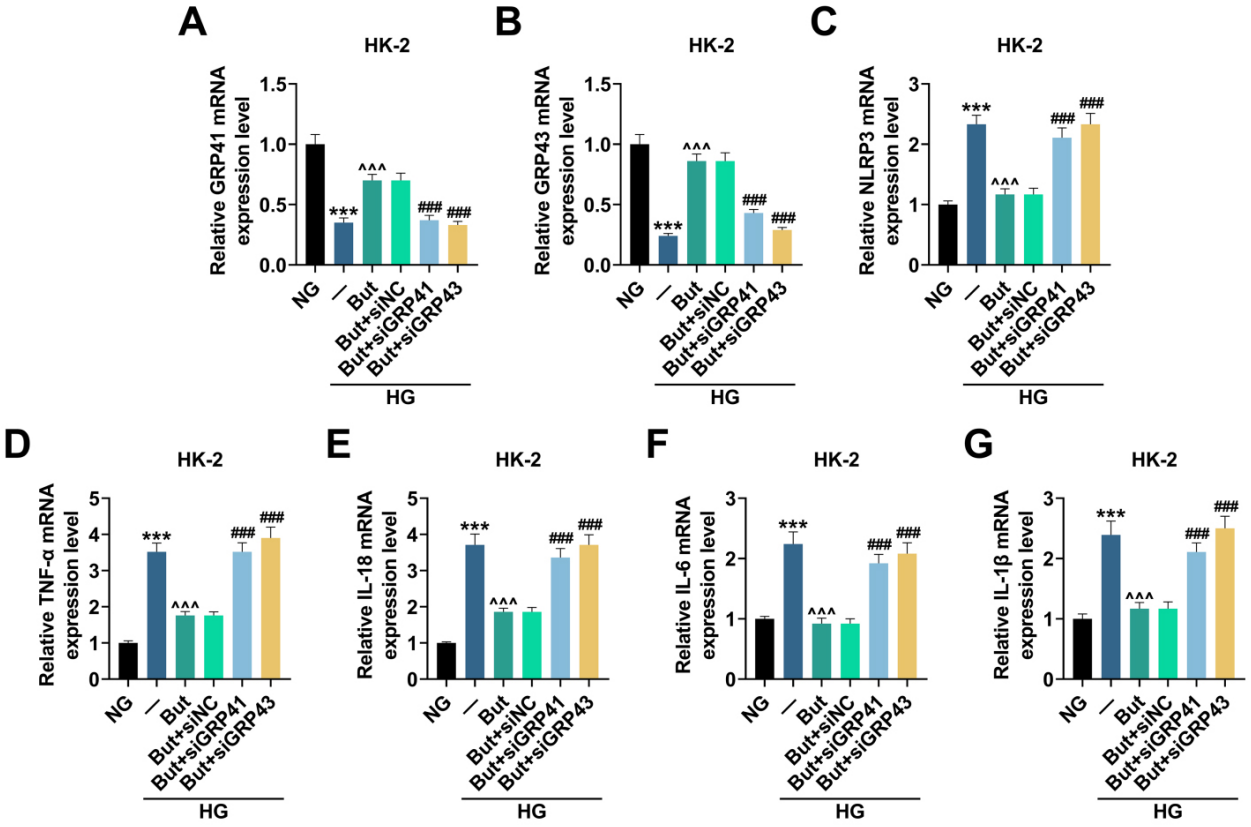

Fig. 2. *GPR41*/*GPR43* silencing reverses the attenuating effect of But in HG-induced *GPR41*/*GPR43* inhibition and NLRP3 inflammasome activation in HK-2 cells. (A–G) Expression levels of *GPR41*, *GPR43*, *NLRP3*, *TNF-α*, *IL-18*, I*L-6*, and *IL-1β* in HK-2 cells transfected with either siNC, si*GPR41*, or si*GPR43*, treated with But for 2 hours, and then stimulated with HG for 24 hours were determined using quantitative real-time polymerase chain reaction, with *GAPDH* as a reference gene. ***$p < 0.001$ vs. NG; $^{\wedge\wedge\wedge}p < 0.001$ vs. HG; $^{\#\#\#}p < 0.001$ vs. HG+But+siNC. n = 3. *GPR41/43*, G-protein-coupled receptor 41/43; But, 8 mmol/L sodium butyrate; HG, 30 mM high glucose; *NLRP3*, NLR family pyrin domain containing 3; NG, 5.6 mM normal glucose; siNC, small interfering RNA negative control; si*GPR41*, small interfering RNA against GPR41; *TNF-α*, tumor necrosis factor-α; *IL-18/6/1β*, interleukin-18/6/1β; *GAPDH*, glyceraldehyde-3-phosphate dehydrogenase.

The 24-hour urine albumin serves as an indicator of renal function affected by hyperglycemia [23]. ELISA results revealed that the 24-hour urine albumin level was significantly higher in the DN group than in the NC group at 11 weeks (Fig. 4A, $p < 0.001$). Treatment with But decreased the 24-hour urine albumin level in DN rats (Fig. 4A, $p < 0.001$), which was counteracted by *GPR41*/*GPR43* silencing (Fig. 4A, $p < 0.001$). Furthermore, serum blood urea nitrogen (BUN) and creatinine levels were measured. BUN and creatinine levels were markedly higher in the DN group compared to the NC group (Fig. 4B,C, $p < 0.001$), indicating kidney injury. Following 12 weeks of But stimulation, BUN and creatinine levels were reduced in the DN+But group compared to the DN group (Fig. 4B,C, $p < 0.001$), but *GPR41*/*GPR43* knockdown reversed this effect (Fig. 4B,C, $p < 0.001$).

Additionally, KW/BW was significantly higher in the DN group than in the NC group (Fig. 4D, $p < 0.001$), indicating kidney hypertrophy. However, KW/BW almost returned to normal levels after But stimulation in the DN+But group (Fig. 4D, $p < 0.001$). *GPR41*/*GPR43* silencing attenuated the effect of But, KW/BW level increased (Fig. 4D, $p < 0.001$).

GPR41/GPR43 Silencing Reverses the Attenuating Effect of But on Renal Morphology Deterioration and EMT in DN Rats

Moreover, kidney tissues were stained with H&E, PAS, and Masson staining methods. Compared to the NC group, rats in the DN group exhibited renal histopathological changes, including an increase in mesangial matrix detected by H&E staining, increased mesangial matrix and basement membrane thickening detected by PAS staining, and collagen deposition and fibrosis detected by Masson staining (Fig. 5A). The renal pathological alterations observed in DN rats were improved by But treatment, while the condition in the DN+But+shGPR41/shGPR43 group was aggravated compared to the DN+But+shNC group

Journal of
BIOLOGICAL REGULATORS
and Homeostatic Agents

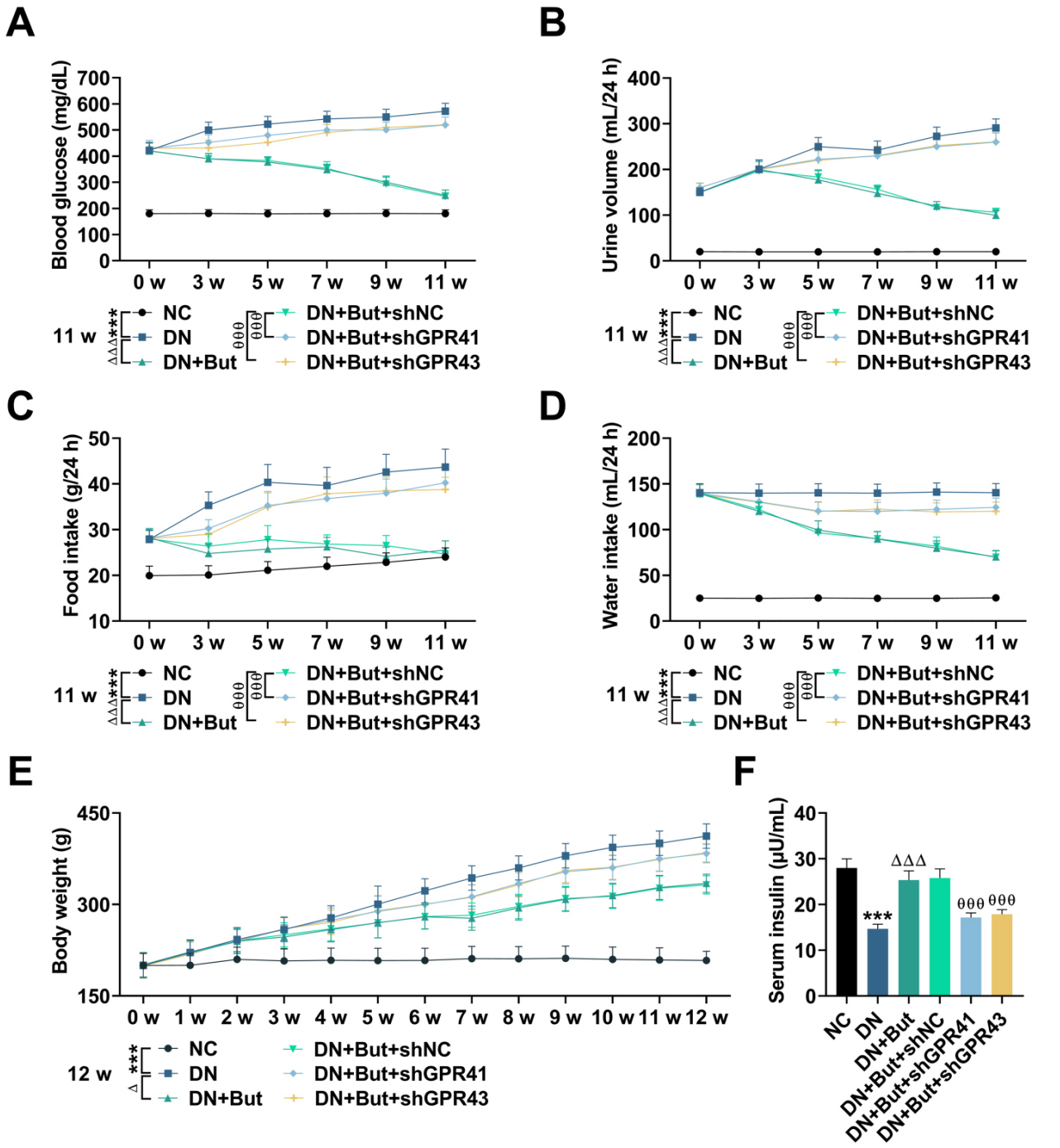

Fig. 3. *GPR41/GPR43* silencing reverses the attenuating effect of But in diabetic symptoms in DN rats. (A–F) Rats were injected with a lentivirus solution to knockdown *GPR41*/*GPR43*, followed by an intraperitoneal injection of STZ, which was performed, and subsequently treated with But for 12 weeks. (A–D) The blood glucose, 24-hour urine volume, 24-hour food intake, and 24-hour water intake of the rats were measured at 0, 3, 5, 7, 9, and 11 weeks post-STZ injection. Blood glucose levels were measured using a blood glucose monitor. (E) The rat body weight was recorded weekly from 0–12 weeks post-STZ injection. (F) Serum insulin levels of the rats were analyzed by ELISA at 12 weeks post-STZ injection. ***$p < 0.001$ vs. NC; $^{\Delta}p < 0.05$, $^{\Delta\Delta\Delta}p < 0.001$ vs. DN; $^{\theta\theta\theta}p < 0.001$ vs. DN+But+shNC. n = 10. *GPR41/43*, G-protein-coupled receptor 41/43; But, 100 mmol/L sodium butyrate; DN, diabetic nephropathy; shNC, short hairpin RNA negative control; shGPR41/43, short hairpin RNA against *GPR41/43*; STZ, 60 mg/kg streptozotocin; ELISA, enzyme-linked immunosorbent assay; NC, normal control.

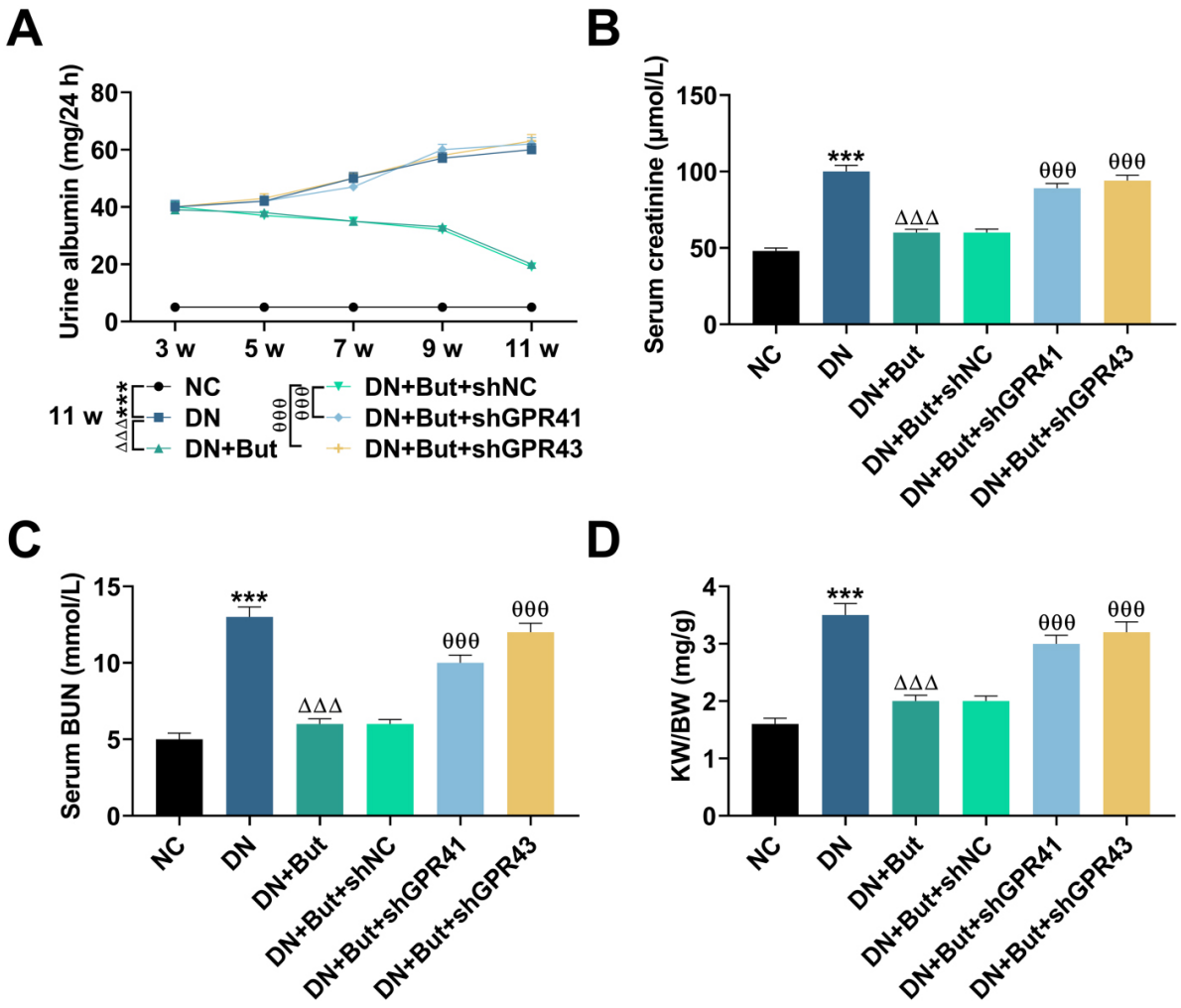

Fig. 4. *GPR41*/*GPR43* silencing reverses the attenuating impact of But in kidney dysfunction in DN rats. (A–D) Rats were injected with lentivirus solution to knock down *GPR41*/*GPR43*, followed by intraperitoneal injection of STZ, and subsequently treated with But for 12 weeks. (A) The 24-hour urine albumin level of the rats was measured using ELISA at 3, 5, 7, 9, and 11 weeks post-STZ injection. (B,C) Serum creatinine and BUN levels of the rats were analyzed by ELISA at 12 weeks post-STZ injection. (D) The KW/BW ratio of the rats was calculated at 12 weeks post-STZ injection. $^{***}p < 0.001$ vs. NC; $^{\Delta\Delta\Delta}p < 0.001$ vs. DN; $^{\theta\theta\theta}p < 0.001$ vs. DN+But+shNC. n = 10. *GPR41*/*43*, G-protein-coupled receptor 41/43; But, 100 mmol/L sodium butyrate; DN, diabetic nephropathy; shNC, short hairpin RNA negative control; shGPR41/43, short hairpin RNA against *GPR41*/*43*; STZ, 60 mg/kg streptozotocin; ELISA, enzyme-linked immunosorbent assay; BUN, blood urea nitrogen; KW/BW, kidney weight/body weight; NC, normal control.

(Fig. 5A). These findings suggest that *GPR41*/*GPR43* silencing reverses the attenuating role of But in deteriorating kidney function and morphology in DN rats.

Furthermore, E-cadherin expression decreased, while α-SMA level increased in rat renal tissues after DN induction (Fig. 5B–D, $p < 0.001$). However, in the renal tissues of DN rats treated with But, E-cadherin expression increased, and the α-SMA expression decreased compared to those in DN rats without But treatment (Fig. 5B–D, $p < 0.001$). Notably, *GPR41*/*GPR43* knockdown partly reversed the effect of But on the expressions of E-cadherin and α-SMA in DN rat renal tissues (Fig. 5B–D, $p < 0.05$).

GPR41/GPR43 Silencing Reverses the Attenuating Effect of But on NLRP3 Inflammasome Activation in Kidney Tissues from DN Rats

In the DN group, compared to the NC group, *GPR41* and *GPR43* were downregulated, while *NLRP3*, *TNF-*α, *IL-18*, *IL-6*, and *IL-1*β were upregulated in kidney tissues from the rats (Fig. 6A–G, $p < 0.001$). Butyrate stimulation increased *GPR41* and *GPR43* levels and decreased *NLRP3*, *TNF-*α, *IL-18*, *IL-6*, and *IL-1*β expressions in kidney tissues from DN rats (Fig. 6A–G, $p < 0.001$), a response that was reversed by *GPR41*/*GPR43* knockdown (Fig. 6A–G, $p < 0.001$). ELISA results revealed that TNF-α, IL-1β,

Journal of
BIOLOGICAL REGULATORS
and Homeostatic Agents

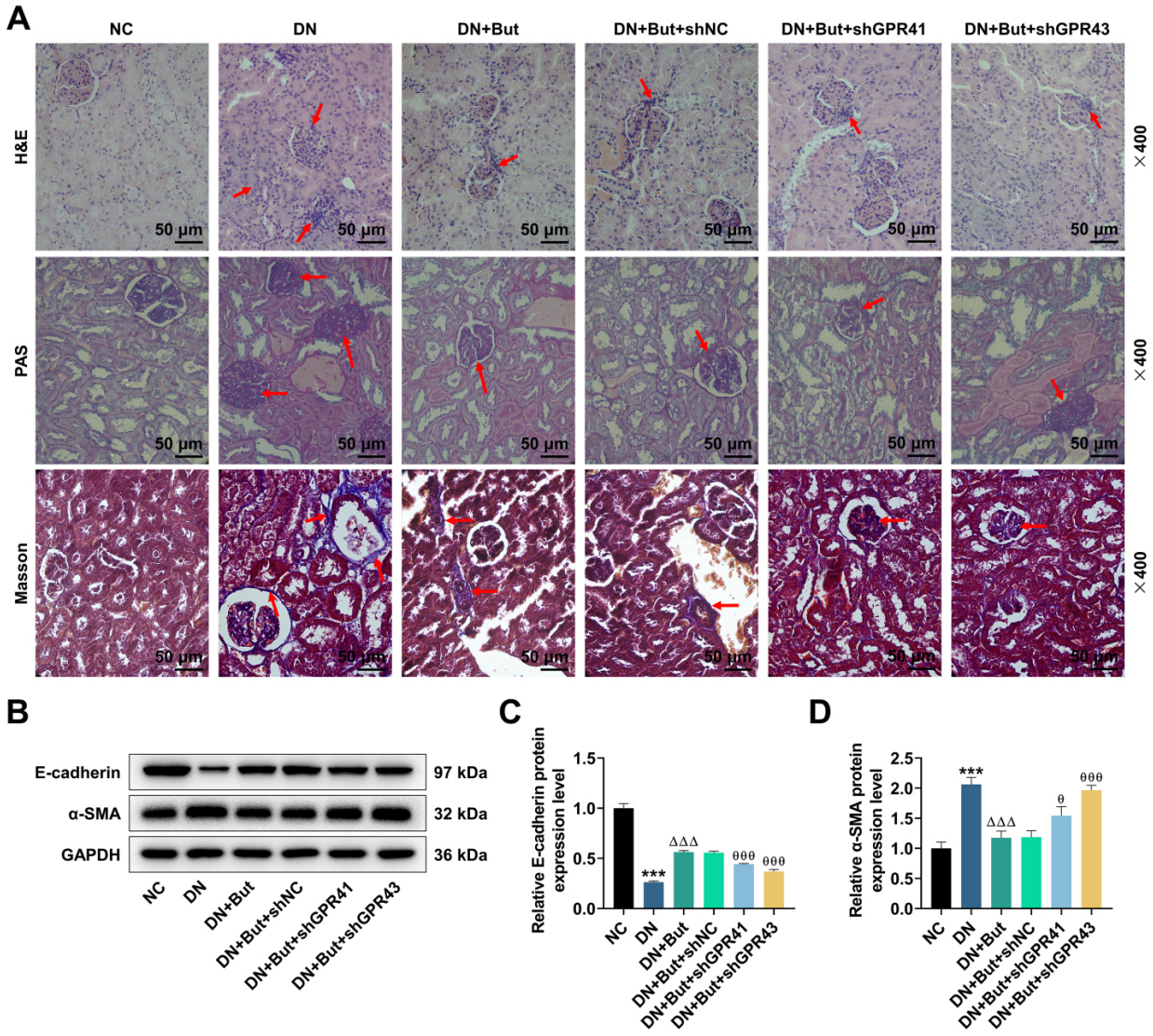

Fig. 5. *GPR41/GPR43* silencing reverses the attenuating effect of But in renal morphology deterioration and EMT in DN rats. (A–D) Rats were injected with lentivirus solution to knock down *GPR41/GPR43*, followed by intraperitoneal injection of STZ, and subsequently treated with But for 12 weeks. (A) The rat renal histopathology of rats was assessed using H&E, PAS, and Masson staining. Scale bar = 50 μm, magnification: ×400. Red arrow indicated the increase in mesangial matrix, basement membrane thickening, and collagen deposition and fibrosis. (B–D) The expressions of EMT-related proteins, including E-cadherin and α-SMA, in rat kidney tissues were determined using Western blot, with GAPDH as an internal standard. ***$p < 0.001$ vs. NC; $^{\Delta\Delta\Delta}p < 0.001$ vs. DN; $^{\theta}p < 0.05$, $^{\theta\theta\theta}p < 0.001$ vs. DN+But+shNC. n = 3. *GPR41/43*, G-protein-coupled receptor 41/43; But, 100 mmol/L sodium butyrate; DN, diabetic nephropathy; shNC, short hairpin RNA negative control; shGPR41/43, short hairpin RNA against *GPR41/43*; STZ, 60 mg/kg streptozotocin; H&E, hematoxylin & eosin; PAS, periodic acid-Schiff; EMT, epithelial-mesenchymal transition; E-cadherin, epithelial cadherin; α-SMA, alpha-smooth muscle actin; NC, normal control.

and IL-18 contents were markedly elevated in kidney tissues from rats in the DN group relative to the NC group (Fig. 6H–J, $p < 0.001$), which was suppressed by But treatment (Fig. 6H–J, $p < 0.001$). *GPR41/GPR43* silencing reversed the effect of But (Fig. 6H–J, $p < 0.001$). Furthermore, immunohistochemistry revealed stronger *NLRP3* expression in the DN group compared to the NC group (Fig. 6K,L, $p < 0.001$). *NLRP3* levels in DN rats were reduced after But stimulation, and *GPR41/GPR43* knockdown counteracted the effect of But (Fig. 6K,L, $p < 0.001$). In summary, *GPR41/GPR43* silencing reverses the attenuating effect of But in NLRP3 inflammasome activation in kidney tissues from DN rats.

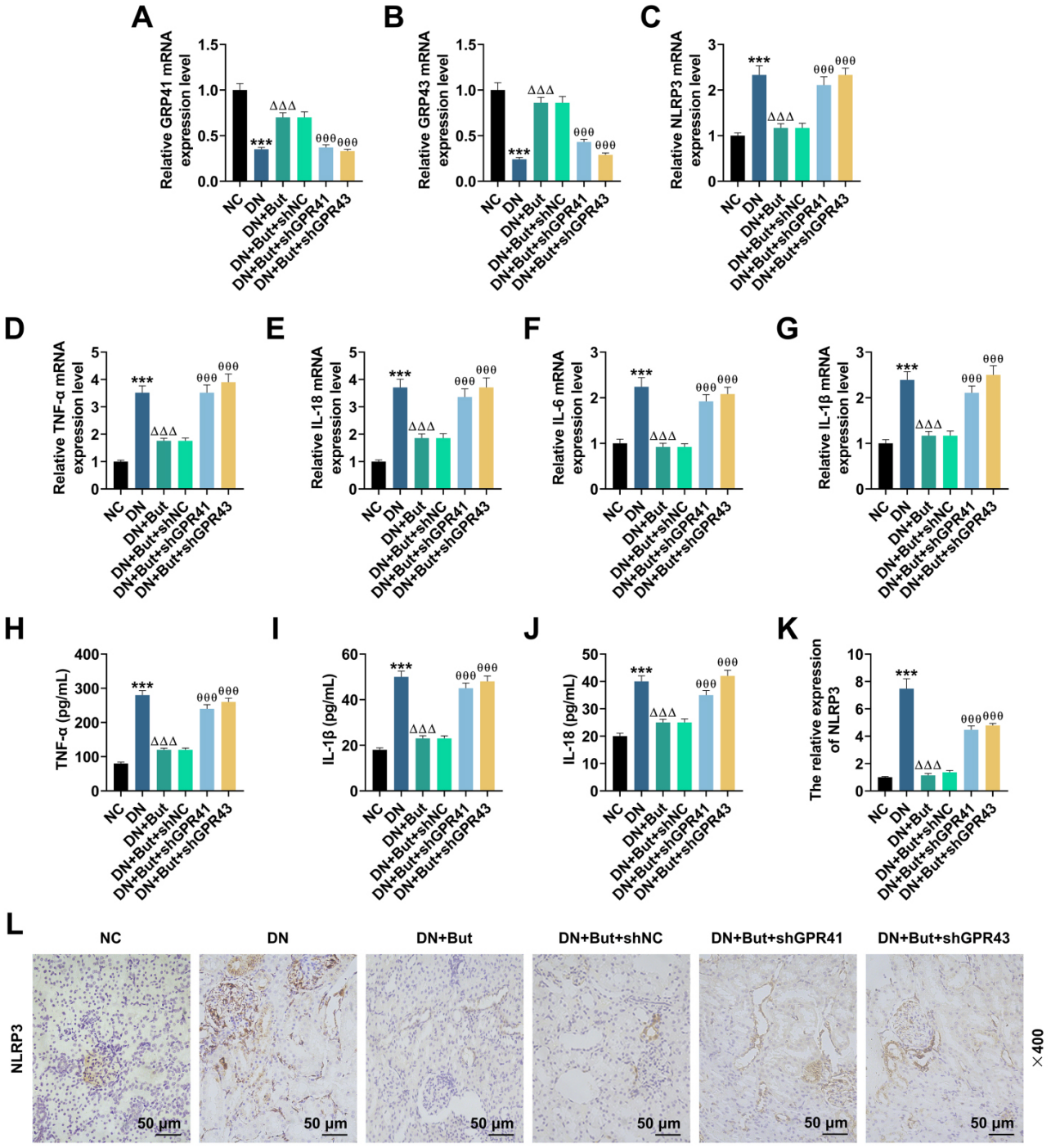

Fig. 6. *GPR41*/*GPR43* silencing reverses the attenuating effect of But on NLRP3 inflammasome activation in kidney tissues from DN rats. (A–G) Rats were injected with lentivirus solution to knock down *GPR41*/*GPR43*, followed by intraperitoneal injection of STZ, and subsequently treated with But for 12 weeks. RT-qPCR was used to measure the expression levels of *GPR41*, *GPR43*, *NLRP3*, *TNF-α*, *IL-18*, *IL-6*, and *IL-1β* in kidney tissues from the rats, with glyceraldehyde-3-phosphate dehydrogenase as a reference gene. (H–J) Enzyme-linked immunosorbent assay was employed to determine the contents of TNF-α, IL-1β, and IL-18 in kidney tissues from the rats. (K,L) Immunohistochemistry was conducted to evaluate the expression of *NLRP3* in kidney tissues from the rats. Scale bar = 50 μm, magnification: ×400. ***$p < 0.001$ vs. NC; $^{\Delta\Delta\Delta}p < 0.001$ vs. DN; $^{\theta\theta\theta}p < 0.001$ vs. DN+But+shNC. n = 3. *GPR41/43*, G-protein-coupled receptor 41/43; But, 100 mmol/L sodium butyrate; NLRP3, NLR family pyrin domain containing 3; DN, diabetic nephropathy; shNC, short hairpin RNA negative control; shGPR41/43, short hairpin RNA against *GPR41/43*; STZ, 60 mg/kg streptozotocin; TNF-α, tumor necrosis factor-α; IL-18/6/1β, interleukin-18/6/1β; NC, normal control.

Journal of
BIOLOGICAL REGULATORS
and Homeostatic Agents

Discussion

Inflammation is a vital contributor to the onset and progression of DN [4]. The NLRP3 inflammasome, as a key mediator of inflammation, contributes to inflammation by activating pro-inflammatory cytokines such as IL-18 and IL-1β. Numerous studies have highlighted the close association between NLRP3 and DN progression [9,25]. HG activates the NLRP3 inflammasome in mesangial cells and renal tubular epithelial cells in the renal cortex, leading to renal tubular epithelial cell apoptosis and contributing to DN progression [26]. Consistent with previous studies, our study observed upregulation of *NLRP3*, *TNF-*α, *IL-18*, *IL-6*, and *IL-1*β in HK-2 cells and in kidney tissues from rats following the induction of DN by HG and STZ.

The role of intestinal microecology in various diseases has garnered significant attention, primarily its association with the onset and progression of DN [27,28]. This association is mediated through the "gut-kidney axis", representing the communication pathway between the kidney and intestinal microbiota [12]. Intestinal flora and its metabolites, such as SCFAs, play a crucial role in regulating the "gut-kidney axis" [29]. SCFAs, including acetate, propionate, and butyrate, are primarily produced by the fermentation of undigested dietary fiber by intestinal flora [30]. Recent research has begun to elucidate the impact of SCFAs on kidney health. For example, acetate has been found to protect the kidney, reduce inflammation, and alleviate renal epithelial cell and immune cell damage in acute kidney injury [31]. SCFAs have also been shown to mitigate DN by inhibiting NF-κB signaling and oxidative stress via mediation through *GPR43* [18]. Additionally, SCFAs suppress NLRP3 inflammasome activation and autophagy, promoting intestinal barrier function and protecting against damage induced by lipopolysaccharide [32].

In our study, Ac, Pr, and But reversed the effects of HG and resisted the impact of STZ on upregulating NLRP3 and related pro-inflammatory cytokines in HK-2 cells and kidney tissues from rats, respectively. Furthermore, the protective effect of SCFAs on DN was evident through reductions in serum creatinine, BUN, urine albumin levels, and KW/BW ratio, as well as improvements in renal morphology [23,33]. Butyrate notably attenuated STZ-induced increases in these indices and abnormalities in rat kidney tissues, aligning with its protective role against DN-related renal injury and dysfunction in previous studies [18]. However, our study did not detect other indicators of urinalysis (nitrite (NIT), glucose, specific gravity (SG), bilirubin (BIL), ketone bodies (KET)), necessitating investigation to elucidate any potential changes in these parameters.

Furthermore, renal fibrosis is a significant hallmark of declining renal function and a fundamental pathological change in DN patients [34]. EMT, and an accumulation of ECM, are the primary drivers of renal fibrogenesis [23,35]. Collagen is a primary component of ECM in kidney tissues [36]. SCFAs protect against renal interstitial fibrosis, reducing the likelihood of DN development [37]. SCFAs also alleviate HG-induced fibrosis in renal tubular epithelial cells [20]. Our study demonstrated that HG and STZ downregulated the epithelial marker E-cadherin and upregulated the mesenchymal cell-expressed molecule α-SMA, a known fibrogenic protein [38], in HK-2 cells and kidney tissues from rats, respectively. Additionally, the renal histopathological changes detected by Masson staining were consistent with renal fibrosis in rats. Consistent with previous findings, these renal fibrosis abnormalities were ameliorated by SCFAs *in vitro* and But *in vivo*.

Moreover, a previous study showed that NLRP3 inflammasome activation promotes the EMT process during fibrosis [39]. SCFAs may signal via GPRs, such as *GPR41* and *GPR43*. SCFAs bind to *GPR41*/*GPR43* to inhibit monocyte chemoattractant protein-1, which is upregulated by TNF-α in human renal cortical epithelial cells, delaying renal inflammatory and fibrotic responses [22]. Based on our findings, But upregulated *GPR41* and *GPR43* to mitigate HG-induced NLRP3 inflammasome activation-mediated inflammation and fibrosis in HK-2 cells. Moreover, SCFAs, especially But, elevate *GPR43* expression to alleviate diabetic symptoms and reduce renal fibrosis and inflammation *in vivo*, preventing and alleviating DN [18]. However, whether SCFAs affect DN-related renal injury and dysfunction *in vivo* via *GPR41*/*GPR43* remains unclear. Our study verified that the renal protection conferred by But in rat DN models was also attributed to the activation of *GPR41*/*43*.

In this study, we observed that But downregulated NLRP3 inflammasome activation in HG-induced HK-2 cells and STZ-stimulated rat kidneys, and this effect was reversed by silencing *GPR41*/*43*. Thus, But inhibited renal NLRP3 inflammasome activation and fibrosis, attenuating DN by activating *GPR41*/*GPR43*. However, this study only used one SCFAs (But) to intervene in DN rats, and did not compare the effects and differences of other SCFAs (such as acetate and propionate), nor did it explore the effects of different doses and durations. Therefore, follow-up studies will continue to explore in depth the relative efficacy and optimal dosage of different SCFAs, as well as possible synergistic or antagonistic effects.

Conclusions

In conclusion, SCFAs inhibit NLRP3 inflammasome activation to alleviate inflammation and EMT in DN through the activation of *GPR41*/*43*. These findings may have significant implications for preventing and treating DN in clinical settings. Notably, this study represents the first investigation into the *GPR41*-related mechanism of SCFAs in DN.

Availability of Data and Materials

The analyzed data sets generated during the study are available from the corresponding authors on reasonable request.

Author Contributions

Substantial contributions to conception and design: NJS; Data acquisition, data analysis and interpretation: KDC, YH, KYW, QL, LPW; Drafting the article or critically revising it for important intellectual content: All authors; Final approval of the version to be published: All authors; Agreement to be accountable for all aspects of the work in ensuring that questions related to the accuracy or integrity of the work are appropriately investigated and resolved: All authors.

Ethics Approval and Consent to Participate

All experiments involving animals were carried out at Zhejiang Baiyue Biotech Co., Ltd. according to the ethical guidelines from the China Council on Animal Care and Use and approved by Ethics Committee of Zhejiang Baiyue Biotech Co., Ltd. (Approval No. ZJBYLA-IACUC-20220601).

Acknowledgment

Not applicable.

Funding

This Project was supported by the Ningbo Natural Science Foundation, China [Grant No.2019A610254]; the Medical Scientific Research Foundation of Zhejiang Province, China [Grant No.2020KY851]; the Project of NINGBO Leading Medical & Health Discipline [Grant No.2022-S03].

Conflict of Interest

The authors declare no conflict of interest.

Supplementary Material

Supplementary material associated with this article can be found, in the online version, at https://doi.org/10.23812/j.biol.regul.homeost.agents.20243806.380.

References

[1] Dong W, Jia C, Li J, Zhou Y, Luo Y, Liu J, *et al*. Fisetin Attenuates Diabetic Nephropathy-Induced Podocyte Injury by Inhibiting NLRP3 Inflammasome. Frontiers in Pharmacology. 2022; 13: 783706.

[2] Chen N, Yang Z, Mu L, Wu M, Song J, Zhou T, *et al*. ChREBP Deficiency Suppresses Renal Inflammation and Fibrosis Via Inhibiting NLRP3 Inflammasome Activation in Diabetic Kidney Disease. Discovery Medicine. 2022; 33: 69–83.

[3] Zhou J, Zhang S, Sun X, Lou Y, Bao J, Yu J. Hyperoside ameliorates diabetic nephropathy induced by STZ via targeting the miR-499-5p/APC axis. Journal of Pharmacological Sciences. 2021; 146: 10–20.

[4] Moreno JA, Gomez-Guerrero C, Mas S, Sanz AB, Lorenzo O, Ruiz-Ortega M, *et al*. Targeting inflammation in diabetic nephropathy: a tale of hope. Expert Opinion on Investigational Drugs. 2018; 27: 917–930.

[5] Nordbø OP, Landolt L, Eikrem Ø, Scherer A, Leh S, Furriol J, *et al*. Transcriptomic analysis reveals partial epithelial-mesenchymal transition and inflammation as common pathogenic mechanisms in hypertensive nephrosclerosis and Type 2 diabetic nephropathy. Physiological Reports. 2023; 11: e15825.

[6] Wada J, Makino H. Innate immunity in diabetes and diabetic nephropathy. Nature Reviews. Nephrology. 2016; 12: 13–26.

[7] Yang M, Wang X, Han Y, Li C, Wei L, Yang J, *et al*. Targeting the NLRP3 Inflammasome in Diabetic Nephropathy. Current Medicinal Chemistry. 2021; 28: 8810–8824.

[8] Williams BM, Cliff CL, Lee K, Squires PE, Hills CE. The Role of the NLRP3 Inflammasome in Mediating Glomerular and Tubular Injury in Diabetic Nephropathy. Frontiers in Physiology. 2022; 13: 907504.

[9] Chen F, Wei G, Xu J, Ma X, Wang Q. Naringin ameliorates the high glucose-induced rat mesangial cell inflammatory reaction by modulating the NLRP3 Inflammasome. BMC Complementary and Alternative Medicine. 2018; 18: 192.

[10] Fu Y, Wu N, Zhao D. Function of NLRP3 in the Pathogenesis and Development of Diabetic Nephropathy. Medical Science Monitor. 2017; 23: 3878–3884.

[11] Iatcu CO, Steen A, Covasa M. Gut Microbiota and Complications of Type-2 Diabetes. Nutrients. 2021; 14: 166.

[12] Hoorn EJ, Zietse R. Gut-kidney kaliuretic signaling: looking forward to feeding. Kidney International. 2015; 88: 1230–1232.

[13] Al Khodor S, Shatat IF. Gut microbiome and kidney disease: a bidirectional relationship. Pediatric Nephrology. 2017; 32: 921–931.

[14] Rukavina Mikusic NL, Kouyoumdzian NM, Choi MR. Gut microbiota and chronic kidney disease: evidences and mechanisms that mediate a new communication in the gastrointestinal-renal axis. Pflugers Archiv: European Journal of Physiology. 2020; 472: 303–320.

[15] Schönfeld P, Wojtczak L. Short- and medium-chain fatty acids in energy metabolism: the cellular perspective. Journal of Lipid Research. 2016; 57: 943–954.

[16] Priyadarshini M, Kotlo KU, Dudeja PK, Layden BT. Role of Short Chain Fatty Acid Receptors in Intestinal Physiology and Pathophysiology. Comprehensive Physiology. 2018; 8: 1091–1115.

[17] Tian X, Zeng Y, Tu Q, Jiao Y, Yao S, Chen Y, *et al*. Butyrate alleviates renal fibrosis in CKD by regulating NLRP3-mediated pyroptosis via the STING/NF-κB/p65 pathway. International Immunopharmacology. 2023; 124: 111010.

[18] Huang W, Man Y, Gao C, Zhou L, Gu J, Xu H, *et al*. Short-Chain Fatty Acids Ameliorate Diabetic Nephropathy via GPR43-Mediated Inhibition of Oxidative Stress and NF-κB Signaling. Oxidative Medicine and Cellular Longevity. 2020; 2020: 4074832.

[19] Tang G, Du Y, Guan H, Jia J, Zhu N, Shi Y, *et al*. Butyrate ameliorates skeletal muscle atrophy in diabetic nephropathy by enhancing gut barrier function and FFA2-mediated PI3K/Akt/mTOR signals. British Journal of Pharmacology. 2022; 179: 159–178.

[20] Li YJ, Ma J, Loh YW, Chadban SJ, Wu H. Short-chain fatty

Journal of
BIOLOGICAL REGULATORS
and Homeostatic Agents

acids directly exert anti-inflammatory responses in podocytes and tubular epithelial cells exposed to high glucose. Frontiers in Cell and Developmental Biology. 2023; 11: 1182570.

[21] Ang Z, Ding JL. GPR41 and GPR43 in Obesity and Inflammation - Protective or Causative? Frontiers in Immunology. 2016; 7: 28.

[22] Kobayashi M, Mikami D, Kimura H, Kamiyama K, Morikawa Y, Yokoi S, *et al*. Short-chain fatty acids, GPR41 and GPR43 ligands, inhibit TNF-α-induced MCP-1 expression by modulating p38 and JNK signaling pathways in human renal cortical epithelial cells. Biochemical and Biophysical Research Communications. 2017; 486: 499–505.

[23] Zhang L, Jing M, Liu Q. Crocin alleviates the inflammation and oxidative stress responses associated with diabetic nephropathy in rats via NLRP3 inflammasomes. Life Sciences. 2021; 278: 119542.

[24] Ding T, Wang S, Zhang X, Zai W, Fan J, Chen W, *et al*. Kidney protection effects of dihydroquercetin on diabetic nephropathy through suppressing ROS and NLRP3 inflammasome. Phytomedicine. 2018; 41: 45–53.

[25] Feng H, Gu J, Gou F, Huang W, Gao C, Chen G, *et al*. High Glucose and Lipopolysaccharide Prime NLRP3 Inflammasome via ROS/TXNIP Pathway in Mesangial Cells. Journal of Diabetes Research. 2016; 2016: 6973175.

[26] Lee WC, Chiu CH, Chen JB, Chen CH, Chang HW. Mitochondrial Fission Increases Apoptosis and Decreases Autophagy in Renal Proximal Tubular Epithelial Cells Treated with High Glucose. DNA and Cell Biology. 2016; 35: 657–665.

[27] Linh HT, Iwata Y, Senda Y, Sakai-Takemori Y, Nakade Y, Oshima M, *et al*. Intestinal Bacterial Translocation Contributes to Diabetic Kidney Disease. Journal of the American Society of Nephrology. 2022; 33: 1105–1119.

[28] Zhao J, Zhang QL, Shen JH, Wang K, Liu J. Magnesium lithospermate B improves the gut microbiome and bile acid metabolic profiles in a mouse model of diabetic nephropathy. Acta Pharmacologica Sinica. 2019; 40: 507–513.

[29] Li L, Ma L, Fu P. Gut microbiota-derived short-chain fatty acids and kidney diseases. Drug Design, Development and Therapy. 2017; 11: 3531–3542.

[30] Primec M, Mičetić-Turk D, Langerholc T. Analysis of short-chain fatty acids in human feces: A scoping review. Analytical Biochemistry. 2017; 526: 9–21.

[31] Andrade-Oliveira V, Amano MT, Correa-Costa M, Castoldi A, Felizardo RJF, de Almeida DC, *et al*. Gut Bacteria Products Prevent AKI Induced by Ischemia-Reperfusion. Journal of the American Society of Nephrology. 2015; 26: 1877–1888.

[32] Feng Y, Wang Y, Wang P, Huang Y, Wang F. Short-Chain Fatty Acids Manifest Stimulative and Protective Effects on Intestinal Barrier Function Through the Inhibition of NLRP3 Inflammasome and Autophagy. Cellular Physiology and Biochemistry. 2018; 49: 190–205.

[33] Abou-Hany HO, Atef H, Said E, Elkashef HA, Salem HA. Crocin mediated amelioration of oxidative burden and inflammatory cascade suppresses diabetic nephropathy progression in diabetic rats. Chemico-Biological Interactions. 2018; 284: 90–100.

[34] Lin YC, Chang YH, Yang SY, Wu KD, Chu TS. Update of pathophysiology and management of diabetic kidney disease. Journal of the Formosan Medical Association. 2018; 117: 662–675.

[35] Ma J, Zhang L, Hao J, Li N, Tang J, Hao L. Up-regulation of microRNA-93 inhibits TGF-β1-induced EMT and renal fibrogenesis by down-regulation of Orai1. Journal of Pharmacological Sciences. 2018; 136: 218–227.

[36] Wang J, Duan L, Gao Y, Zhou S, Liu Y, Wei S, *et al*. Angiotensin II receptor blocker valsartan ameliorates cardiac fibrosis partly by inhibiting miR-21 expression in diabetic nephropathy mice. Molecular and Cellular Endocrinology. 2018; 472: 149–158.

[37] Li YJ, Chen X, Kwan TK, Loh YW, Singer J, Liu Y, *et al*. Dietary Fiber Protects against Diabetic Nephropathy through Short-Chain Fatty Acid-Mediated Activation of G Protein-Coupled Receptors GPR43 and GPR109A. Journal of the American Society of Nephrology. 2020; 31: 1267–1281.

[38] Li R, Guo Y, Zhang Y, Zhang X, Zhu L, Yan T. Salidroside Ameliorates Renal Interstitial Fibrosis by Inhibiting the TLR4/NF-κB and MAPK Signaling Pathways. International Journal of Molecular Sciences. 2019; 20: 1103.

[39] Peng L, Wen L, Shi QF, Gao F, Huang B, Meng J, *et al*. Scutellarin ameliorates pulmonary fibrosis through inhibiting NF-κB/NLRP3-mediated epithelial-mesenchymal transition and inflammation. Cell Death & Disease. 2020; 11: 978.